Organic Electronics 37 (2016) 148–154

Contents lists available at ScienceDirect

Organic Electronics

journal homepage: www.elsevier.com/locate/orgel

Radical polymers improve the metal-semiconductor interface in organic field-effect transistors

Seung Hyun Sung [a], Nikhil Bajaj [b], Jeffrey F. Rhoads [b], George T. Chiu [b], Bryan W. Boudouris [a, *]

[a] 480 Stadium Mall Drive, School of Chemical Engineering, Purdue University, West Lafayette, IN 47907, United States
[b] 585 Purdue Mall, School of Mechanical Engineering, Purdue University, West Lafayette, IN 47907, United States

ARTICLE INFO

Article history:
Received 27 April 2016
Received in revised form
7 June 2016
Accepted 14 June 2016

Keywords:
PTMA
Pentacene
OFET
Organic-metal interface
Inkjet printing
Radical polymer

ABSTRACT

Modifying the organic-metal interface in organic field-effect transistors (OFETs) is a critical means by which to improve device performance; however, to date, all of the interfacial modifying layers utilized in these systems have been closed-shell in nature. Here, we introduce open-shell oxidation-reduction-active (redox-active) macromolecules, namely radical polymers, in order to serve as interfacial modifiers in pentacene-based OFETs. Through careful selection of the chemistry of the specific radical polymer, poly(2,2,6,6-tetramethylpiperidine-1-oxyl methacrylate) (PTMA), the charge transport energy level of the interfacial modifying layer was tuned to provide facile charge injection and extraction between the pentacene active layer and the gold source and drain electrodes of the OFET. The inclusion of this radical polymer interlayer, which was deposited in through straightforward inkjet printing, led to bottom-contact, bottom-gate OFETs with significantly increased mobility and ON/OFF current ratios relative to OFETs without the PTMA interlayer. The underlying mechanism for this improvement in device performance is explained in terms of the charge transport capability at the organic-metal interface and with respect to the pentacene grain growth on the radical polymer. Thus, this effort presents a new, open-shell-based class of materials for interfacial modifying materials, and describes the underlying physics behind the practical operation of these materials.

1. Introduction

Organic field-effect transistors (OFETs) have emerged as promising alternatives to their inorganic counterparts in applications where mechanical durability, low-cost, and high-throughput manufacturing of devices are of larger import than rapid charge carrier transport (*e.g.*, $\mu > 10$ cm^2 V^{-1} s^{-1}) and fast device response (*i.e.*, $f > 10$ MHz) [1]. As with many organic electronic architectures, interfaces play a critical role in determining the overall performance of the devices [2–5]. In particular, the metal-semiconductor [6] and metal-dielectric [7,8] interfaces in OFETs are crucial in allowing the organic semiconductor active layer material to achieve its full performance ability. As such, a significant amount of effort has been placed in finding suitable materials, processing conditions, and deposition techniques for the interfacial optimization. Through these myriad attempts, the electronic and structural properties of the interfaces can be manipulated towards the desired device response [9,10]. One of the most implemented techniques with respect to modifying the metal-semiconductor interface is the insertion of a thin layer between the metal and semiconductor layers. The specific material of interest can range from self-assembled monolayers (SAMs) [10–15] of electrically-insulating species to electrically-conductive conjugated polymers [16,17] [*e.g.,* poly(3,4-ethylene dioxythiophene) doped with poly(styrene sulfonate) (PEDOT:PSS)]. In all of these instances, however, the organic interlayer has always consisted of molecules with closed-shell designs. Here, we alter this archetype through the introduction of an open-shell molecule and radical polymer, poly(2,2,6,6-tetramethylpiperidine-1-oxyl methacrylate) (PTMA), as a thin interfacial modifying layer.

In the majority of previous efforts, radical polymers, which are generally composed of a non-conjugated backbone and pendant groups bearing stable radicals, have been mainly utilized in electrolyte-supported energy storage applications (*e.g.,* organic radical batteries) [18–23]. However, in more recent efforts, the

* Corresponding author.
E-mail address: boudouris@purdue.edu (B.W. Boudouris).

http://dx.doi.org/10.1016/j.orgel.2016.06.020
1566-1199/

unique charge transport mechanism, which involves oxidation-reduction (redox) reactions between pendant stable radical groups, has attracted growing interest in solid-state organic electronic applications [24–27]. That is, PTMA has risen to the fore of these organic electronic applications due to the robust nitroxide radicals that can be oxidized to the oxoammonium cation or reduced to the aminoxyl anion in a rather rapid manner even in devices that do not contain a supporting electrolyte [28]. Specifically, the preference of PTMA to be oxidized to the cation state (in a manner analogous to that typically associated with p-type transport in conjugated organic electronic systems) and its Singularly Occupied Molecular Orbital (SOMO) energy transport level of ~5.2 eV removed from vacuum make it compatible as a hole charge carrier pathway with many well-studied small molecule and macromolecular conjugated organic semiconducting materials [29,30]. These molecular advantages, combined with the critical need to tune the interfacial properties in organic field-effect transistors, provide one of the great potentials for radical polymers to impact the thin film transistor design paradigm.

In order to demonstrate the synergy of radical polymers and conjugated organic semiconducting materials in organic electronic devices, we fabricated pentacene-based OFETs in the bottom-gate, bottom-contact geometry (Fig. 1a). In these devices, a thin film of PTMA was inserted between the bottom contact gold source and drain electrodes and the thermally-evaporated pentacene semiconducting active layer. Importantly, the PTMA thin film was deposited in a high-throughput manner, with high spatial resolution, using an advanced inkjet printing technique. In this way, the PTMA interlayer was deposited only between the gold electrodes and the pentacene semiconductor (i.e., PTMA was not present in the active OFET channel as shown in Fig. 1b). The insertion of this radical polymer interlayer improved the ON/OFF current ratio and the hole mobility value of the pentacene-based OFETs relative to OFETs that did not contain a PTMA interlayer. This improvement in device performance is tied to the enhancement of the interfacial charge injection and extraction properties of the PTMA layer (manifested by a reduced contact resistance at the optimized PTMA thin film thickness) and the fact that the presence of the PTMA layer positively influenced the crystalline nature of the pentacene thin film. Furthermore, by controlling the concentration of the inkjet-deposited polymer solution, the thicknesses of the PTMA thin films could be readily controlled. This led to an optimal PTMA film thickness, which balanced the relatively poor electrical-conducting properties of PTMA (compared to gold) and the positive impact of the interlayer, which is in charge of the electronic and structural properties of pentacene at the metal-organic interface. In this manner, the results presented below demonstrate the first application of a radical polymer as the interfacial layer in an OFET device and highlight its potential as an interfacial modifying material; furthermore, it stresses the critical design rules for incorporating open-shell materials into field-effect transistors.

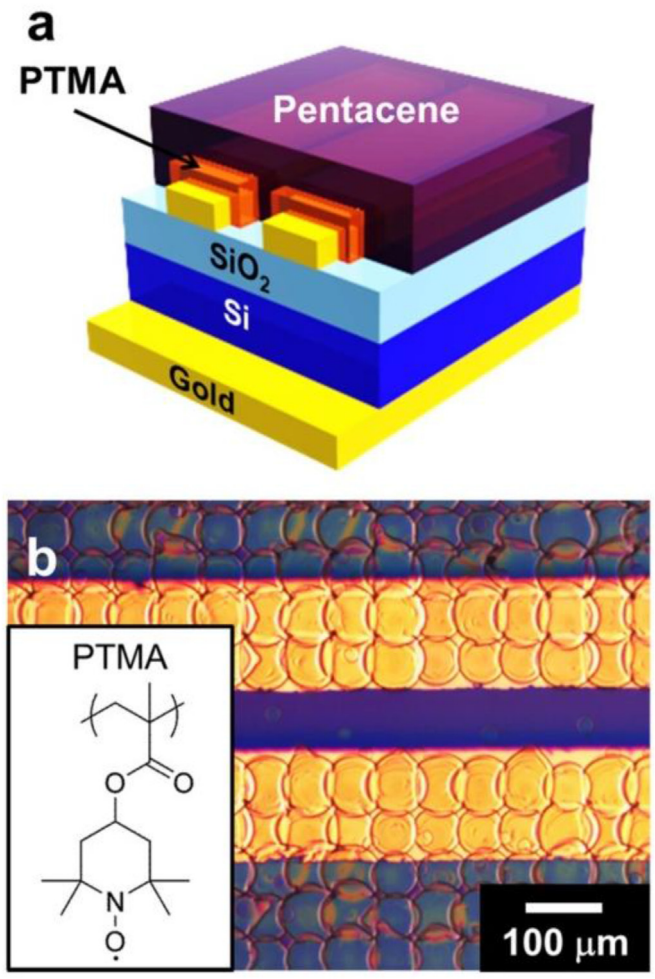

Fig. 1. (a) Schematic depiction of the pentacene-based OFET with a PTMA interlayer between the metal contact and the organic semiconductor. (b) Optical microscope image of inkjet-printed PTMA droplets on the gold source and drain electrodes. Note that the resolution of the inkjet printing process allows for the deposition of the PTMA only above the gold contacts and not in the channel of the OFET (i.e., the SiO_2 region between two electrodes). The chemical structure of PTMA is inset.

2. Experimental

2.1. OFET fabrication

PTMA (M_n ~11 kg mol^{-1}, $Đ$ ~1.3) was synthesized using a reversible addition-fragmentation chain transfer (RAFT) polymerization, and the radical density along the PTMA (i.e., after conversion from the closed-shell to the open-shell form) was ~80% [29]. In order to generate the solutions for thin film casting, PTMA was dissolved in toluene at a desired concentration, and the solution was stirred for 1 day prior to printing. Note that the overlap concentration for PTMA in toluene was estimated to be ~5 mg mL^{-1}. Pentacene (≥99.9%) was purchased from Sigma-Aldrich and used as received. Pentacene-based OFETs that included PTMA interlayers between the metal and organic layers were fabricated as typical bottom-gate, bottom-contact devices. As shown in Fig. 1a, a *p*-doped silicon wafer and gold were used as the substrate and back gate electrode, respectively. The silicon substrate was insulated from the pentacene semiconductor through the deposition of a 300 nm-thick layer of SiO_2 gate dielectric (C = 11 nF cm^{-2}). The Si/SiO_2 wafer substrate was sonicated in acetone, chloroform, and isopropyl alcohol in a sequential manner. After drying under nitrogen gas, 3 nm of titanium (Ti), which was used as an adhesion layer, and 50 nm of gold (Au) were evaporated in order to serve as the source and drain electrodes. Then, the PTMA solution was printed using an inkjet technique at positions only on the source and drain electrodes (Fig. 1b). Specifically, the PTMA arrays were created by a thermal droplet ejection system coupled with a motorized XY stage (HP TIPS Inkjet System mounted above an Anorad WKY XY Positioning Stage). The printer readily delivered droplets of PTMA dissolved in toluene, and, after evaporation of the toluene solvent, the printing resulted in a ~100 μm spot size on the substrate. The deposition process was performed at ambient conditions and without applying any heat to the substrate or nozzle. Finally, a 70 nm pentacene active layer was evaporated onto the

patterned PTMA substrates as well as the SiO_2 surface between the two electrodes. In order to compare these devices with the base case, pentacene was deposited on the gold electrodes without the PTMA layer at the interface of the pentacene and the gold electrodes. In these cases, the SiO_2 was treated with hexamethyldisilazane (HMDS) (Sigma-Aldrich) in order to create a stable CH_3-terminated surface, as previously reported [14,15]. Specifically, HMDS was spin-coated at 3,000 rpm for 30 s, and then the substrate was baked at 100 °C for 30 min. The bottom contact OFET was tested with a channel length (L) and width (W) of 100 μm and 10 mm, respectively. The electrical characterization data reported here were based on the average measurements of more than 12 devices for each specific condition. To elucidate the impact of PTMA on contact resistance, OFETs with four different channel lengths L (0.1 mm, 4.1 mm, 4.7 mm, 8.7 mm) were fabricated and tested at fixed width $W = 10$ mm. And the width normalized contact resistance (R_C) is obtained from the intercept of the total resistance (R_T) vs. L plot at $L = 0$.

2.2. Device measurements and structural characterization

All current-voltage characteristics of the OFETs were acquired using a Keithley 2400 source meter while testing under vacuum in an inert atmosphere probe station (Lakeshore) at T ~20 °C. The thicknesses and surface morphologies were characterized by an atomic force microscopy (AFM, Veeco Dimension 3100). Also, the crystalline nature of the thin films were evaluated using grazing incidence x-ray diffraction (GI-XRD) in the range of $1\ nm^{-1} < q < 22\ nm^{-1}$ using a Rigaku SmartLab diffractometer.

3. Results and discussion

Fig. 1a shows a schematic OFET structure with the PTMA interlayer. The gold/heavily-doped Si wafer acts as the gate electrode while the SiO_2 (300 nm) serves as the gate dielectric. The inkjet-printed PTMA is used as the interfacial modifying layer between the semiconducting pentacene and the gold source/drain electrodes. Importantly, the inkjet printing was designed to ensure that the PTMA interlayer did not span across the length of the OFET channel (*i.e.*, to prevent the PTMA from causing a short between the two gold electrodes), as shown in Fig. 1b. This approach was used because inkjet-printing is a facile way to deposit an organic droplet on a defined target [31]; therefore it allows for simple and fast insertion of PTMA layer on the top of gold electrodes.

The inclusion of the PTMA layer significantly improves the performance of the pentacene-based OFETs. Fig. 2 shows the output curves [*i.e.*, the drain current (I_D) versus the drain voltage (V_D)] and the transfer curves [*i.e.*, the drain current (I_D) versus the gate voltage (V_G)] of an OFET without a PTMA interlayer and another OFET with a PTMA interlayer (with a thickness of 8 nm) that was deposited from a 3 mg mL^{-1} toluene solution. As shown in the Supporting Information (Fig. S1), the performance metrics of the OFETs are related to the quality of the pentacene-metal interface and not the charge transport ability of PTMA, as pristine (*i.e.*, not doped) PTMA of itself is a relatively poor conductor compared to gold. In fact, the PTMA interlayer drastically enhanced the charge carrier (hole) mobility and ON/OFF current ratio of the pentacene-based OFET devices. The electrical performances of two types of OFETs are summarized in Table 1. The pentacene OFETs fabricated

Table 1
Summary of OFET performance without PTMA layer and with PTMA layer.

OFET structure	μ_{max} [$cm^2\ V^{-1}\ s^{-1}$]	μ_{avg} [$cm^2\ V^{-1}\ s^{-1}$]	$I_{On}/I_{Off(avg)}$	R_C [Ω cm]
No PTMA	5.8×10^{-3}	5.0×10^{-3} (±0.001)[a]	~10^2	1.2×10^6
PTMA (8 nm)	7.6×10^{-2}	6.3×10^{-2} (±0.008)[a]	~10^5	2.1×10^5

[a] The standard deviation in the measurements from the average. This is based on the measurement of 12 devices.

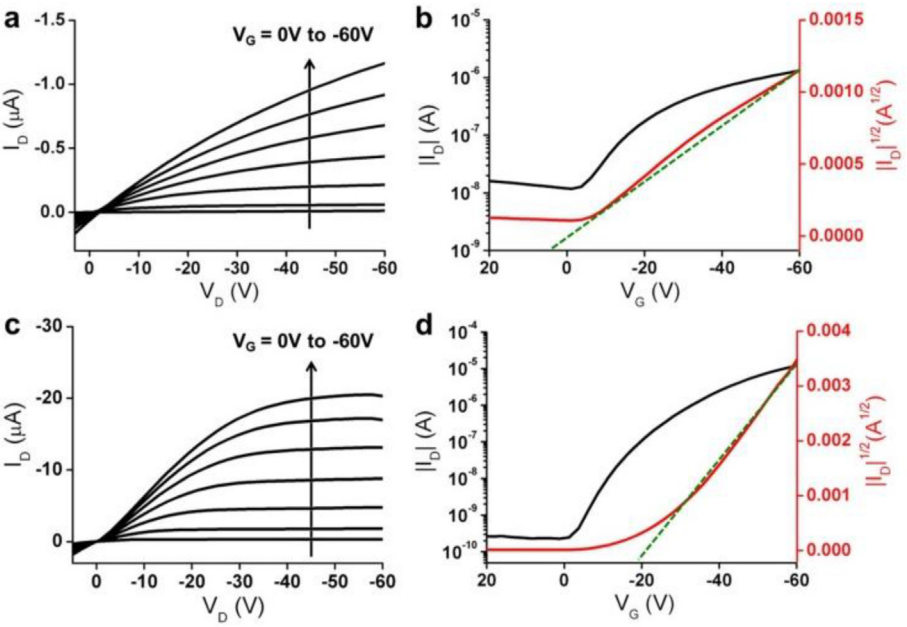

Fig. 2. Representative (a) output characteristics (I_D-V_D) and (b) transfer characteristics (I_D-V_G) of pentacene-based OFET devices without a PTMA interlayer. Representative (c) output and (d) transfer characteristics of pentacene-based OFET devices with 8 nm of PTMA deposited between the organic semiconductor and the gold electrodes. The transfer curves shown in parts (b) and (d) were acquired at a gate voltage of $V_G = -60$ V.

without the PTMA layer have an average hole mobility (μ_{avg}) of 5.0×10^{-3} cm^2 V^{-1} s^{-1} and an ON/OFF current ratio (I_{ON}/I_{OFF}) of ~10^2. On the other hand, insertion of the PTMA layer improved the OFET mobility by an order of magnitude (6.3×10^{-2} cm^2 V^{-1} s^{-1}) and the ON/OFF performance by three orders of magnitude (*i.e.*, to ~10^5).

The field-effect mobility of high performance highly-purified pentacene-based OFET has been shown to be > 0.1 cm^2 V^{-1} s^{-1} [32], but OFETs using singly-sublimed pentacene (like the type used here) and bottom-contact configuration OFET geometries generally show a drop in performance due to contact resistance and hole injection problems [11–13,17,33–36]. By surmounting this limitation, compared to the unmodified gold (*i.e.*, 0 nm of PTMA) OFET, the OFET with the optimized PTMA interlayer exhibited slightly higher ON current values and drastically lower OFF current values, as shown in Fig. 2. Particularly, the OFF current suppression occurs due to an improvement of interfacial transport between gold and pentacene in bottom-contact configuration [14]. As such, the optimized PTMA interlayer successfully facilitates the charge injection between gold and pentacene, as well as the increased hole mobility at the channel region related to higher ON current.

Various concentrations of the PTMA solutions were evaluated in order to establish the optimal radical polymer coating thickness (Fig. 3). To reveal the relationship between the interlayer thickness and the pentacene-based OFET performance, the thickness of the PTMA droplet as a function of concentration was also measured using atomic force microscopy (Fig. S2). The inkjet-printed PTMA layer is relatively thick, compared to spin-coated films made from the same concentration as well as thin monolayer modifying layers (*i.e.*, like the HMDS treatment used for reference OFET device). Therefore, the controlled concentration of PTMA solution plays an important role in charge transport during OFET operation. Usually, relatively thick films can hinder the charge transport between electrodes and the main semiconducting channel in bottom-contact configurations. In this work, a thick PTMA film (*i.e.*, t > 40 nm) can disturb the charge injection from the gold electrode to the pentacene due to the relatively low conductivity of the PTMA compared to gold (Fig. 3a). At a printing solution concentration of 3 mg mL^{-1}, an 8 nm–thick PTMA layer is formed, and the OFETs fabricated using this PTMA thickness showed the optimal performance. In short, this thickness struck a balance between the interfacial positive effects and the relatively low electrical conductivity of PTMA.

This interfacial impact of the PTMA interlayer can be interpreted in a manner that calls for the analysis of the contact resistance of the devices, and the contact resistance values of the devices were obtained using the transfer line method [37–40]. In order to calculate the contact resistance between electrodes and active layer, OFETs with four different channel lengths L (0.1 mm, 4.1 mm, 4.7 mm, 8.7 mm) were fabricated at the fixed width $W = 10$ mm. At a relatively low drain voltage (V_D), the contact resistance at the interface between electrodes and channel layer R_C was determined by extrapolating the plot of total general resistance (R_T) versus channel length to a zero channel length ($L = 0$) using the following equation.

$$R_T = \frac{V_D}{I_D} = R_{Ch} \cdot L + R_C \quad (1)$$

Here, R_{Ch} is the channel resistance per unit length. The representative plot of R_T as a function of L is presented in Fig. S3. As shown in the width-normalized contact resistance (Fig. 3b), the PTMA decreased the contact resistance (relative to a direct pentacene-gold contact) by nearly an order of magnitude. This significant reduction of contact resistance directly impacts the

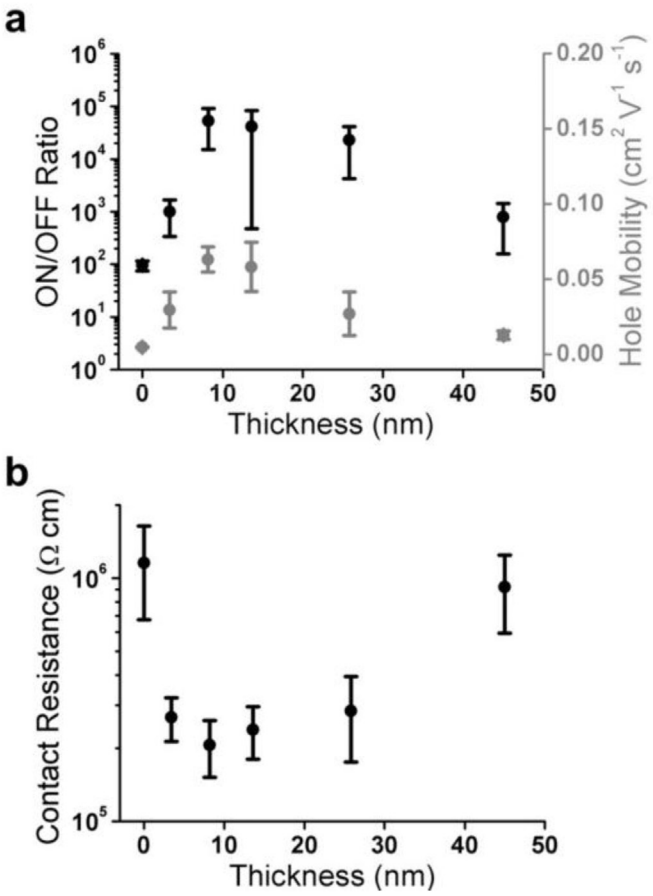

Fig. 3. (a) ON/OFF current ratios (black symbols) and hole mobility values (grey symbols) for the pentacene-based OFETs as a function of the thickness of PTMA interlayer. The data points mark the average value and the error bars indicate one standard deviation. (b) Analysis of contact resistances as a function of the thickness of PTMA interlayer. These width-normalized contact resistances were calculated at a gate voltage of $V_G = -60$ V. These data were calculated over 12 devices.

OFET performance. Compared to device performances in Fig. 3a, it is clear that the low contact resistance produces the high ON/OFF ratio as well as the high hole carrier mobility. However, the contact resistance is also affected by PTMA thickness. Therefore, according to the application of PTMA interlayers into organic field-effect transistors, monitoring the relative thickness of these materials is one of the critical design parameters in the overall device landscape.

The reasons for this positive electrode modifying behavior in this pentacene-based OFET are diverse, yet they are readily explained. First, the alignment of the SOMO energy level of PTMA relative to the work function of the metal and the transport level of the organic semiconductor allows for the facile transport of holes between the gold and pentacene layers. This is important because the performance of an OFET device depends on the energy barriers that control the charge transport at the interface of two layers. Generally, there is a mismatch between the work function of gold (ϕ_{Au} ~5.1 eV) and the HOMO level of pentacene, which leads to a hole injection barrier of up to ~0.5 eV–1.0 eV, according to various reports in the literature [41–44]. This mismatch is believed to originate from interfacial chemical reactions or the orientation of molecular dipoles at the metal-semiconductor interface [2,43,44]. On the other hand, at the interface of gold and pentacene, PTMA prevents the gold layer from undesired electrical interactions and chemical contamination, and it also serves as a means by which to

transport charges towards the active channel. Furthermore, the PTMA is an environmentally and electrically resilient material [45], and its SOMO level is known to reside at ~5.2 eV removed from vacuum [30], which is between the charge transport energy levels of gold and pentacene. Therefore, the placement of the PTMA thin film at the interface of gold and pentacene lowers the hole injection barrier, resulting in enhanced charge carrier mobility and higher ON/OFF performance.

In addition to purely electronic effects, PTMA also impacts the pentacene grain structure. As shown in Fig. 4, PTMA significantly improved the pentacene film quality with respect to the grain size and the overall film root mean square (RMS) roughness. That is, the PTMA layer causes the nucleation and growth of larger-sized pentacene grains than what is achieved when the pentacene is deposited on bare gold. Interestingly, this structure-altering result reported here for thin films of pentacene has been reported for poly(methyl methacrylate) (PMMA) buffer layers as well [33,46]. Therefore, it would be consistent with the idea that the glassy nature and methacrylate-based backbone of PTMA may affect the observed OFET response; however, PTMA is clearly differentiated from PMMA in the fact that it is electrically-active. This is why relatively thick film (26 nm) of PTMA, compared to PMMA (8 nm), can be used as an OFET interlayer. As previously reported with a PEDOT:PSS interlayer in pentacene-based OFETs [17], the thickness effect on device performance is smaller when using conductive interlayers than when using insulating buffer layers. Thus, the utilization of PTMA could lead to a higher degree of reproducibility when scaling the transistor fabrication process. Additionally, in a manner that is different than the use of the PMMA buffer layer, the PTMA reduced the apparent surface roughness of the pentacene thin film when this value is measured over the same area. This effect originates from the amorphous and smooth surface of pristine PTMA film (Fig. S4). Over more than 10 devices, it was established that the roughness of PTMA droplet rim does not impede the grain growth of pentacene film. The reduction in film roughness has been tied to the reduction in defect trap sites [14]. As such, this is one of the great potentials of PTMA in OFET applications. In Fig. 4a and b, the reduced surface roughness of the pentacene surface (RMS roughness for the bare gold is 18.8 nm and the RMS roughness for a PTMA-modified substrate is 6.15 nm) is clearly presented when the evaporation rate of pentacene was held constant at 0.3 Å s^{-1}. This result supports the idea that the interface of pentacene and gold would also be smooth. Correspondingly, this reduction in the number of defect trap sites is closely related to the lower OFF current state with a low gate leakage, resulting in the enhanced I_{ON}/I_{OFF} ratio, as presented in Fig. 2.

The grazing-incidence x-ray diffraction (GI-XRD) measurements in Fig. 5, reveal that the crystallinity of the pentacene film is increased when it was grown on PTMA relative to the bare gold substrate. Both films display the same primary peak, which is the thin film phase (001) parallel to the surface. When evaporated onto the PTMA film, the pentacene molecules exhibit significantly improved thin film phase peak intensities as compared to the bare gold substrate. In fact, crystallite sizes can be calculated to be 83 nm for the pentacene film grown on PTMA and 63 nm for the film

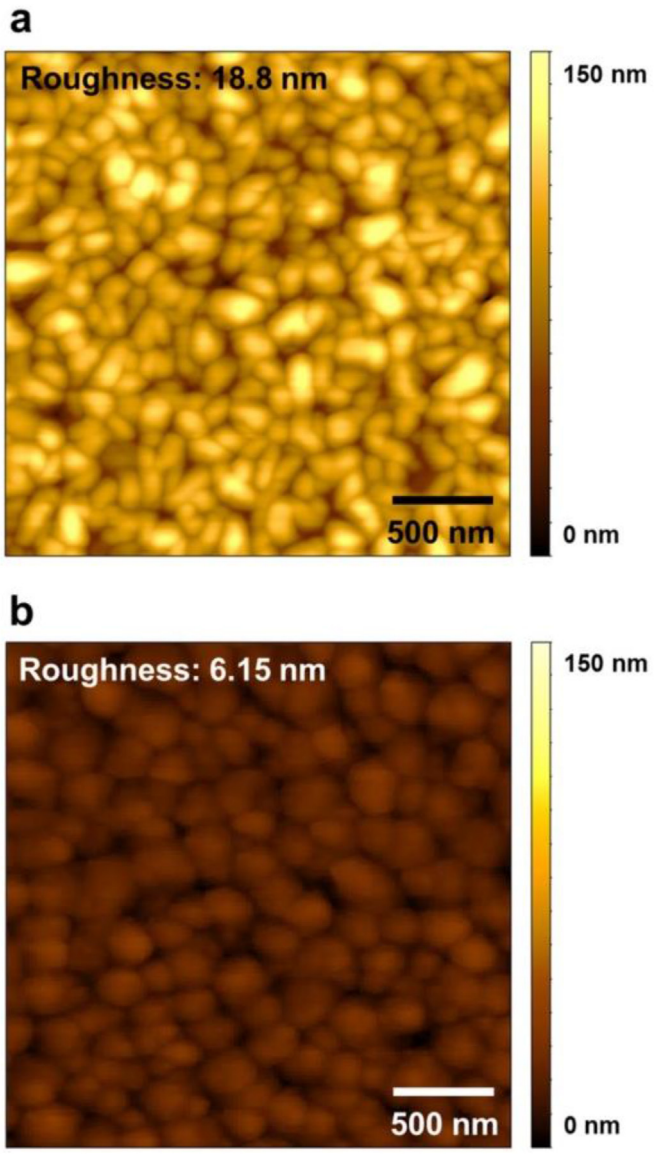

Fig. 4. Atomic force microscopy (AFM) surface topography images of pentacene on (a) bare gold and (b) on a PTMA thin film. Larger grains are present in (b) relative to (a), and the surface roughness of the thin film in (b) is also significantly lower than that measured in (a).

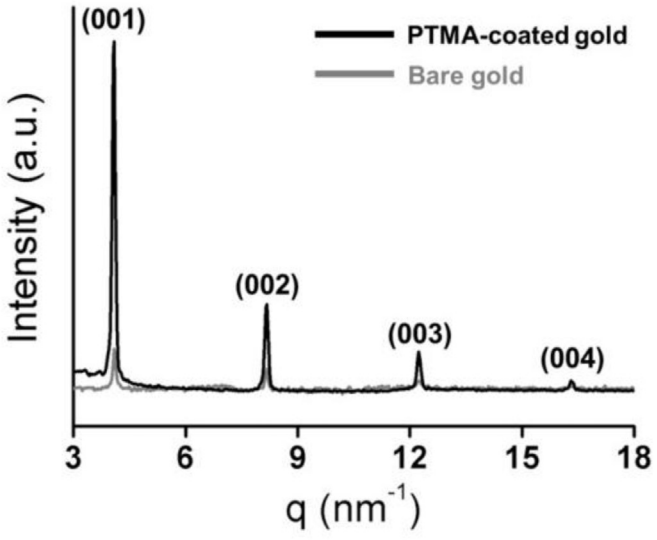

Fig. 5. GI-XRD patterns of pentacene on PTMA-coated gold (black) and on bare gold (grey). The increased intensity (i.e., decrease in the full-width half-maximum (FWHM) values) of the reflections observed in the PTMA-coated sample highlight the improved relative degree of crystallinity of channel layer when the pentacene is evaporated onto the PTMA contacts as opposed to the bare gold contacts.

grown directly onto the gold substrate, according to the Scherrer equation (with $K_s = 0.95$, which is commonly used for organic semiconductors) [47]. This combined increase in relative crystallinity and crystallite size corresponds well with the electrical performance of the OFET devices, and these data demonstrate how the PTMA interlayer can be used to manipulate both the electronic and structural properties of the organic semiconductor. In addition, the surface quality of the metal electrode was improved after PTMA deposition even in case of 1 mg mL^{-1} (t ~3 nm) as presented Fig. 3. As thicker layers of PTMA were deposited, the surface properties became more like those of PTMA and less like those of the pristine gold. In this manner, it is inferred that the grain growth of pentacene, which is critical for OFET performance, was improved with optimal PTMA layer thickness.

4. Conclusion

In summary, a thin layer of the radical polymer PTMA was inserted between the metallic electrode and organic semiconducting layer in bottom-gate, bottom-contact, pentacene-based OFETs using an inkjet printing process. This inkjet printing process allows for the facile deposition of well-defined PTMA thin films that were present only on the surface of the metallic contacts and not within the relatively narrow (~100 μm) channel space. Due to the unique electronic properties, charge transport interactions, and the amorphous nature of the PTMA modifying layer, the performance of the pentacene-based OFET was improved relative to the device that was fabricated with pristine gold electrodes. This was reflected in increased ON/OFF current ratios in the devices and higher hole mobility values for the pentacene-based OFETs, and a decrease in the contact resistance of the OFETs was observed as well. These positive performance metrics are correlated to the SOMO energy level of conductive PTMA and the ability to manipulate the thin film crystalline structure of pentacene. Therefore, this first systematic investigation of PTMA layer in solid state organic field-effect transistors offers one of the novel pathways for the design of radical polymers as an interfacial layer in leading organic electronic devices.

Acknowledgements

We gratefully acknowledge financial support from the Air Force Office of Scientific Research (AFOSR) (Award Number: FA9550-15-1-0449, Program Manager: Dr. Charles Lee). We also like to acknowledge support from Hewlett-Packard for the use of its Thermal Inkjet PicoJet Systems (TIPS).

Appendix A. Supplementary data

Supplementary data related to this article can be found at http://dx.doi.org/10.1016/j.orgel.2016.06.020.

References

[1] G. Horowitz, Organic field-effect transistors, Adv. Mater 10 (1998) 365–377.
[2] H. Ishii, K. Sugiyama, E. Ito, K. Seki, Energy level alignment and interfacial electronic structures at organic/metal and organic/organic interfaces, Adv. Mater 11 (1999) 605–625.
[3] X. Crispin, V. Geskin, A. Crispin, J. Cornil, R. Lazzaroni, W.R. Salaneck, J.L. Bredas, Characterization of the interface dipole at organic/metal interfaces, J. Am. Chem. Soc. 124 (2002) 8131–8141.
[4] N. Koch, Organic electronic devices and their functional interfaces, Chemphyschem 8 (2007) 1438–1455.
[5] H. Ma, H.L. Yip, F. Huang, A.K.Y. Jen, Interface engineering for organic electronics, Adv. Funct. Mater 20 (2010) 1371–1388.
[6] S.W. Rhee, D.J. Yun, Metal-semiconductor contact in organic thin film transistors, J. Mater. Chem. 18 (2008) 5437–5444.
[7] J. Veres, S. Ogier, G. Lloyd, D. de Leeuw, Gate insulators in organic field-effect transistors, Chem. Mater. 16 (2004) 4543–4555.
[8] A. Facchetti, M.H. Yoon, T.J. Marks, Gate dielectrics for organic field-effect transistors: new opportunities for organic electronics, Adv. Mater. 17 (2005) 1705–1725.
[9] D. Braga, G. Horowitz, High-performance organic field-effect transistors, Adv. Mater 21 (2009) 1473–1486.
[10] S. Kobayashi, T. Nishikawa, T. Takenobu, S. Mori, T. Shimoda, T. Mitani, H. Shimotani, N. Yoshimoto, S. Ogawa, Y. Iwasa, Control of carrier density by self-assembled monolayers in organic field-effect transistors, Nat. Mater 3 (2004) 317–322.
[11] I. Kymissis, C.D. Dimitrakopoulos, S. Purushothaman, High-performance bottom electrode organic thin-film transistors, IEEE Trans. Electron. Devices 48 (2001) 1060–1064.
[12] D.J. Gundlach, L.L. Jia, T.N. Jackson, Pentacene TFT with improved linear region characteristics using chemically modified source and drain electrodes, IEEE Electron. Device. L. 22 (2001) 571–573.
[13] B.H. Hamadani, D.A. Corley, J.W. Ciszek, J.M. Tour, D. Natelson, Controlling charge injection in organic field-effect transistors using self-assembled monolayers, Nano Lett. 6 (2006) 1303–1306.
[14] I. Yagi, K. Tsukagoshi, Y. Aoyagi, Modification of the electric conduction at the pentacene/SiO_2 interface by surface termination of SiO_2, Appl. Phys. Lett. 86 (2005) 103502.
[15] J.B. Koo, S.H. Kim, J.H. Lee, C.H. Ku, S.C. Lim, T. Zyung, The effects of surface treatment on device performance in pentacene-based thin film transistor, Synth. Met. 156 (2006) 99–103.
[16] R. Schroeder, L.A. Majewski, M. Grell, J. Maunoury, J. Gautrot, P. Hodge, M. Turner, Electrode specific electropolymerization of ethylenedioxythiophene: injection enhancement in organic transistors, Appl. Phys. Lett. 87 (2005) 113501.
[17] K. Hong, S.Y. Yang, C. Yang, S.H. Kim, D. Choi, C.E. Park, Reducing the contact resistance in organic thin-film transistors by introducing a PEDOT : PSS hole-injection layer, Org. Electron. 9 (2008) 864–868.
[18] K. Nakahara, S. Iwasa, M. Satoh, Y. Morioka, J. Iriyama, M. Suguro, E. Hasegawa, Rechargeable batteries with organic radical cathodes, Chem. Phys. Lett. 359 (2002) 351–354.
[19] H. Nishide, K. Oyaizu, Materials science - toward flexible batteries, Science 319 (2008) 737–738.
[20] T. Suga, H. Ohshiro, S. Sugita, K. Oyaizu, H. Nishide, Emerging N-Type redox-active radical polymer for a totally organic polymer-based rechargeable battery, Adv. Mater 21 (2009) 1627–1630.
[21] K. Oyaizu, H. Nishide, Radical polymers for organic electronic devices: a radical departure from conjugated polymers? Adv. Mater 21 (2009) 2339–2344.
[22] K. Nakahara, K. Oyaizu, H. Nishide, Organic radical battery approaching practical use, Chem. Lett. 40 (2011) 222–227.
[23] T. Janoschka, M.D. Hager, U.S. Schubert, Powering up the future: radical polymers for battery applications, Adv. Mater 24 (2012) 6397–6409.
[24] Y. Yonekuta, K. Susuki, K.C. Oyaizu, K.J. Honda, H. Nishide, Battery-inspired, nonvolatile, and rewritable memory architecture: a radical polymer-based organic device, J. Am. Chem. Soc. 129 (2007) 14128–14129.
[25] E.P. Tomlinson, M.E. Hay, B.W. Boudouris, Radical polymers and their application to organic electronic devices, Macromolecules 47 (2014) 6145–6158.
[26] L. Rostro, L. Galicia, B.W. Boudouris, Suppressing the environmental dependence of the open-circuit voltage in inverted polymer solar cells through a radical polymer anodic modifier, J. Polym. Sci. Pol. Phys. 53 (2015) 311–316.
[27] A.J. Wingate, B.W. Boudouris, Recent advances in the syntheses of radical-containing macromolecules, J. Polym. Sci. Part A Polym. Chem. 54 (2016) 1875–1894.
[28] L. Rostro, S.H. Wong, B.W. Boudouris, Solid state electrical conductivity of radical polymers as a function of pendant group oxidation state, Macromolecules 47 (2014) 3713–3719.
[29] L. Rostro, A.G. Baradwaj, B.W. Boudouris, Controlled radical polymerization and quantification of solid state electrical conductivities of macromolecules bearing pendant stable radical groups, ACS Appl. Mater. Interfaces 5 (2013) 9896–9901.
[30] A.G. Baradwaj, L. Rostro, M.A. Alam, B.W. Boudouris, Quantification of the solid-state charge mobility in a model radical polymer, Appl. Phys. Lett. 104 (2014) 213306.
[31] B.J. de Gans, P.C. Duineveld, U.S. Schubert, Inkjet printing of polymers: state of the art and future developments, Adv. Mater 16 (2004) 203–213.
[32] H.E. Katz, Z. Bao, The physical chemistry of organic field-effect transistors, J. Phys. Chem. B 104 (2000) 671–678.
[33] F. De Angelis, S. Cipolloni, L. Mariucci, G. Fortunato, High-field-effect-mobility pentacene thin-film transistors with polymethylmetacrylate buffer layer, Appl. Phys. Lett. 86 (2005) 203505.
[34] K. Ihm, B. Kim, T.H. Kang, K.J. Kim, M.H. Joo, T.H. Kim, S.S. Yoon, S. Chung, Molecular orientation dependence of hole-injection barrier in pentacene thin film on the Au surface in organic thin film transistor, Appl. Phys. Lett. 89 (2006) 033504.
[35] T. Maeda, H. Kato, H. Kawakami, Organic field-effect transistors with reduced contact resistance, Appl. Phys. Lett. 89 (2006) 123508.
[36] C.A. Di, G. Yu, Y.Q. Liu, X.J. Xu, D.C. Wei, Y.B. Song, Y.M. Sun, Y. Wang, D.B. Zhu, J. Liu, X.Y. Liu, D.X. Wu, High-performance low-cost organic field-effect transistors with chemically modified bottom electrodes, J. Am. Chem. Soc. 128 (2006) 16418–16419.

[37] P.V. Necliudov, M.S. Shur, D.J. Gundlach, T.N. Jackson, Contact resistance extraction in pentacene thin film transistors, Solid State Electron 47 (2003) 259–262.
[38] H. Klauk, G. Schmid, W. Radlik, W. Weber, L.S. Zhou, C.D. Sheraw, J.A. Nichols, T.N. Jackson, Contact resistance in organic thin film transistors, Solid State Electron 47 (2003) 297–301.
[39] J. Zaumseil, K.W. Baldwin, J.A. Rogers, Contact resistance in organic transistors that use source and drain electrodes formed by soft contact lamination, J. Appl. Phys. 93 (2003) 6117–6124.
[40] E.J. Meijer, G.H. Gelinck, E. van Veenendaal, B.H. Huisman, D.M. de Leeuw, T.M. Klapwijk, Scaling behavior and parasitic series resistance in disordered organic field-effect transistors, Appl. Phys. Lett. 82 (2003) 4576–4578.
[41] N.J. Watkins, L. Yan, Y.L. Gao, Electronic structure symmetry of interfaces between pentacene and metals, Appl. Phys. Lett. 80 (2002) 4384–4386.
[42] R. Schroeder, L.A. Majewski, M. Grell, A study of the threshold voltage in pentacene organic field-effect transistors,, Appl. Phys. Lett. 83 (2003) 3201–3203.
[43] N.J. Watkins, Y. Gao, Vacuum level alignment of pentacene on LiF/Au, J. Appl. Phys. 94 (2003) 1289–1291.
[44] K. Hong, J.W. Lee, S.Y. Yang, K. Shin, H. Jeon, S.H. Kim, C. Yang, C.E. Park, Lower hole-injection barrier between pentacene and a 1-hexadecanethiol-modified gold substrate with a lowered work function, Org. Electron 9 (2008) 21–29.
[45] A.G. Baradwaj, L. Rostro, B.W. Boudouris, On the environmental and electrical bias stability of radical polymer conductors in the solid state, Macromol. Chem. Phys. 213 (2016) 477–484.
[46] T.S. Huang, Y.K. Su, P.C. Wang, Study of organic thin film transistor with polymethylmethacrylate as a dielectric layer, Appl. Phys. Lett. 91 (2007) 092116.
[47] R. Matsubara, M. Sakai, K. Kudo, N. Yoshimoto, I. Hirosawa, M. Nakamura, Crystal order in pentacene thin films grown on SiO_2 and its influence on electronic band structure, Org. Electron. 12 (2011) 195–201.